

PREPARED FOR SUBMISSION TO JINST

13<sup>TH</sup> WORKSHOP ON RESISTIVE PLATE CHAMBERS AND RELATED  
DETECTORS,  
22–26 FEBRUARY 2016,  
GHENT UNIVERSITY, BELGIUM

# Numerical study on the effect of design parameters and spacers on RPC signal and timing properties

---

**A. Jash,<sup>a,c,1</sup> N. Majumdar,<sup>a</sup> S. Mukhopadhyay,<sup>a</sup> S. Saha<sup>a</sup> and S. Chattopadhyay<sup>b</sup>**

<sup>a</sup>*Applied Nuclear Physics Division, Saha Institute of Nuclear Physics, Kolkata, India*

<sup>b</sup>*Experimental High Energy Physics Division, Variable Energy Cyclotron Centre, Kolkata, India*

<sup>c</sup>*Experimental High Energy Physics Division, Homi Bhabha National Institute, Mumbai, India*

*E-mail:* [abhik.jash@saha.ac.in](mailto:abhik.jash@saha.ac.in)

**ABSTRACT:** Numerical calculations have been performed to understand the reason for the observed non-uniform response of a Resistive Plate Chamber (RPC) in a few critical regions such as near edge spacers and corners of the device. In this context, the signal from a RPC due to the passage of muons through different regions has been computed. Also, a simulation of RPC timing properties is presented along with the effect of the applied field, gas mixture and geometrical components.

**KEYWORDS:** Resistive-plate chambers; Detector modelling and simulations II (electric fields, charge transport, multiplication and induction, pulse formation, electron emission, etc)

ARXIV EPRINT: [1605.02154](https://arxiv.org/abs/1605.02154)

---

<sup>1</sup>Corresponding author.

---

## Contents

<b>1</b>	<b>Introduction</b>	<b>1</b>
<b>2</b>	<b>Experiment and Simulation Methodologies</b>	<b>2</b>
<b>3</b>	<b>Result</b>	<b>3</b>
3.1	RPC Signal	3
3.2	RPC Timing Properties	4
<b>4</b>	<b>Conclusion</b>	<b>6</b>

---

## 1 Introduction

The India-based Neutrino Observatory (INO) [1], the proposed underground laboratory facility in India will host a magnetized Iron CALorimeter (ICAL) to conduct precise measurements of neutrino oscillation related parameters by studying atmospheric neutrinos. A stack of Resistive Plate Chambers (RPC) in the ICAL detector will provide the timing and 3D spatial information of passing muons, produced in the interaction of the atmospheric neutrinos with the iron layers. About 30,000 RPCs of dimension  $2\text{ m} \times 2\text{ m}$  will be deployed in the ICAL setup. In the last few years, a good amount of R&D effort has been delivered on various issues related to the performance optimization of ICAL. An observation of reduced response towards the edges and corners of the RPC [2] has been regarded as a major motivation for the present work.

Numerical simulation is a good tool to investigate the different processes behind the operation of the detector to analyze the experimental results. This can also be used to optimize different design parameters to improve the detector performance. In the present study, the signal induced on the readout strips for the passage of muons through the RPC has been simulated. To study the effect of the device geometry, the signal has been computed at different regions of the device for different voltages. Some of the results have been compared to actual measurements to validate the calculation procedure. An appropriate approach for this study would be to find out the signal in the presence of a dynamic electric field as the space charges created in the avalanche process tend to modify it [3]. Also the time dependence of the electric field owing to the finite bulk resistivity of the RPC plate should be taken into account in order to carry out an extensive signal simulation. However, the present work involves calculations assuming a static electric field configuration where the RPC is described as a multi-dielectric planar capacitor.

Accurate timing information from the RPC layers of the ICAL setup will help identifying the direction of the passing muon tracks. The parameters of importance in the timing performance of RPC are the average signal arrival time and the time resolution, which in turn

rely upon the electric field configuration of the device and the gas mixture used. In this work, the variation of timing properties of a RPC with the applied voltage has been studied. In order to study the effects of the device, the simulation has been carried out generating the timing response for several critical regions. The dependence on the gas mixture has been investigated through simulations with different  $\text{SF}_6$  concentrations. This component of the gas mixture is known to be important for restricting the streamer mode activity. The results have been compared to measurements wherever available.

The experimental setup and a brief description of the numerical methods are presented in section 2. Section 3 is dedicated to the discussion of the results and the final remarks are made in section 4.

## 2 Experiment and Simulation Methodologies

One bakelite RPC of dimension  $30 \text{ cm} \times 30 \text{ cm}$  with 2 mm gas gap has been operated with a gas mixture of R-134A and Isobutane in 95 : 5 ratio. The schematic diagram of the experimental setup used for carrying out the measurements of the RPC and timing properties is shown in figure 1. A finger scintillator of width 4 cm has been placed aligned with one of the RPC readout strips.

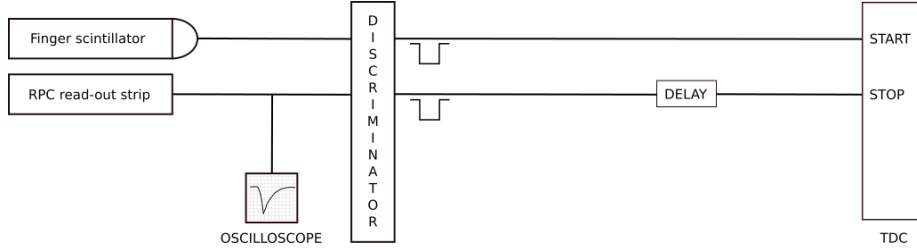


**Figure 1.** Schematic diagram of the experimental setup for RPC signal and timing measurements.

In our numerical simulation, a bakelite RPC of dimension  $30 \text{ cm} \times 30 \text{ cm}$  has been modelled as described in [4]. The Garfield [5] simulation framework has been used to calculate the signal and timing properties of RPC along with its toolkits like neBEM [6], HEED [7] and Magboltz [8] performing different stages of the calculation. neBEM is used to calculate the electrostatic field map, while HEED computes the primary ionization produced by the relativistic charged particles in the gas mixture. The transport properties of electrons in the gas mixture are generated by Magboltz and finally Garfield simulates the drift of primary and avalanche electrons to produce the current induced on readout strips due to the movement of this charge cloud. The field in the gas chamber has been produced by applying bias voltage across the readout panels, to overcome some technical restrictions discussed in [4].

The timing properties of the RPC have been computed by passing 2 GeV muons with incidence angle varying randomly in the range  $0^\circ - 10^\circ$  through a region away from any imperfection (regular region). The passage of a muon track triggers an avalanche of electrons and ions which move towards respective electrodes and induce currents on the readout strips. The current signals for the passage of 5000 muons have been calculated using Garfield. The

average signal arrival time and the time resolution were determined as the mean and RMS, respectively, of the distribution of the time corresponding to the crossing of 20% of the signal amplitude. The same calculations have been performed setting different threshold values in the range 10% - 50% of the signal amplitude. No significant dependence on the threshold value has been observed except for a shift in the average signal arrival time towards higher values for higher thresholds, which is obvious from the fact that higher current values appear at a later time. Small fluctuations in the currents have been observed at very small values of time which has been avoided by using an optimum threshold set to 20% of signal amplitude. In the present study, no effect of ion movements or electronics has been considered.

### 3 Result

#### 3.1 RPC Signal

A typical signal waveform as seen on an oscilloscope, due to the passage of muons through the RPC is shown in figure 2(a). Figure 2(b) shows a typical signal waveform as calculated

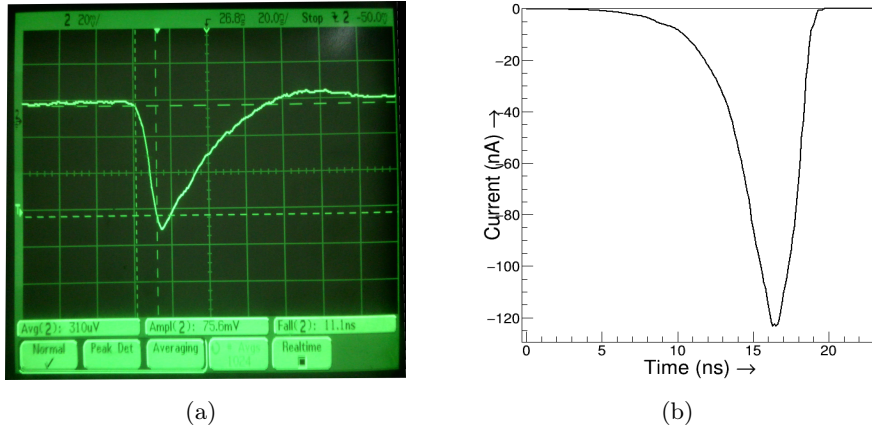


**Figure 2.** (a) Typical RPC signal on an oscilloscope, (b) Simulated signal waveform (average of 50 events).

numerically for the passage of 2 GeV muons at an angle  $5^\circ$  with the vertical direction. As neither the effect of ion movement nor the electronics have been taken into account, only the rising edge of the signal of 7 ns has been compared with the experimental form with a rise time of 11 ns. To see the effect of edge spacers, 100 muons with 2 GeV energy have been sent through a regular region and regions near the edge. The waveform of signals averaged over the 100 events in those regions have been calculated and are shown in figure 3 for two different voltages. It can be seen that the amplitude of the signal falls as one approaches the edge spacer which is obvious as the electric field suffers from an edge effect [4]. Consequently, the loss of response at those regions can lead to less efficient or dead regions near the edges of the RPC.

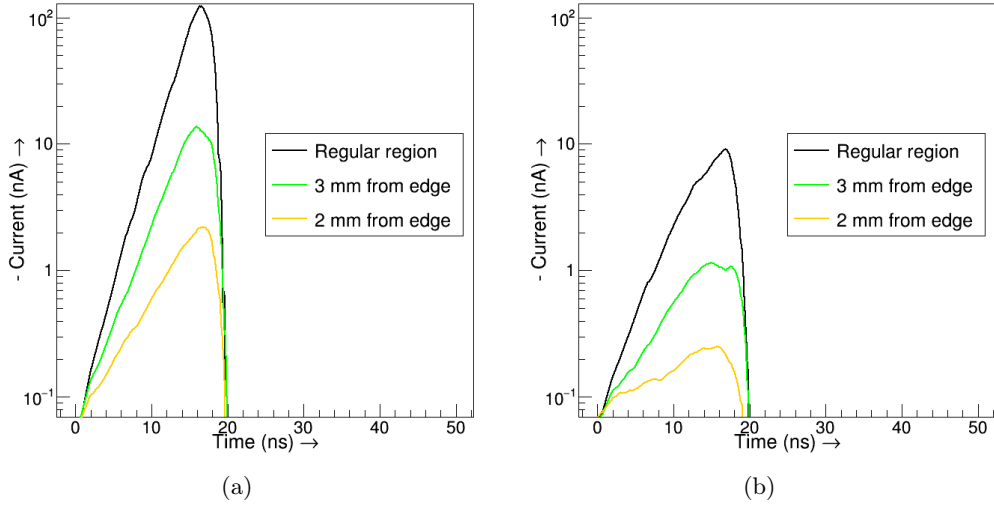


**Figure 3.** Average signal induced due to the passage of 100 muons of energy 2 GeV through different regions of the RPC for the voltages (a) 8.6232 kV and (b) 8.3381 kV across the coats.

### 3.2 RPC Timing Properties

The typical TDC spectra measured for two different voltages are shown in figure 4. The mean and the RMS values of the histogram give the average signal arrival time and the time resolution respectively. The variation of average signal arrival time and time resolution

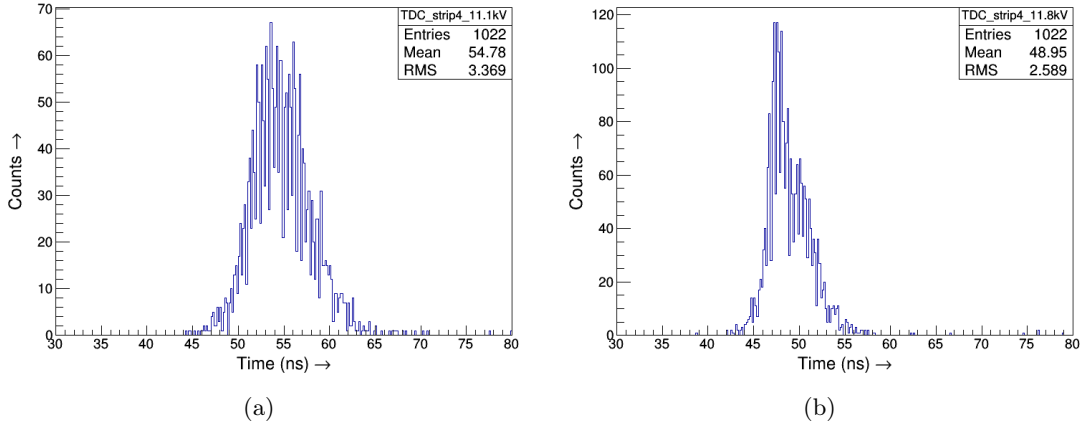


**Figure 4.** Typical TDC spectra of RPC when the applied voltage is (a) 11.1 kV, (b) 11.8 kV.

with the applied voltage is shown in figure 5. The numerical calculation of the same quantities is shown in figure 6. Both the average signal arrival time and time resolution of the RPC decrease with increasing field, as the values of the drift velocity of electrons ( $V_z$ ) and the effective Townsend co-efficient increase with the field, which follows from the relation of time resolution to these parameters discussed in [9]. The variation of these two gas parameters for the gas mixture R-134A : Isobutane = 95 : 5 with the increase in electrostatic field, as calculated using Magboltz is shown in figure 7.

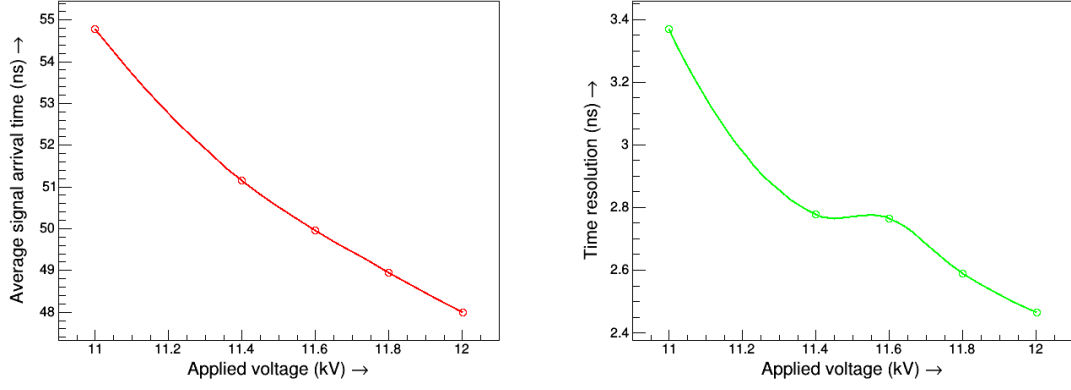


**Figure 5.** Variation of average signal arrival time and RPC time resolution with applied voltage from experimental data.

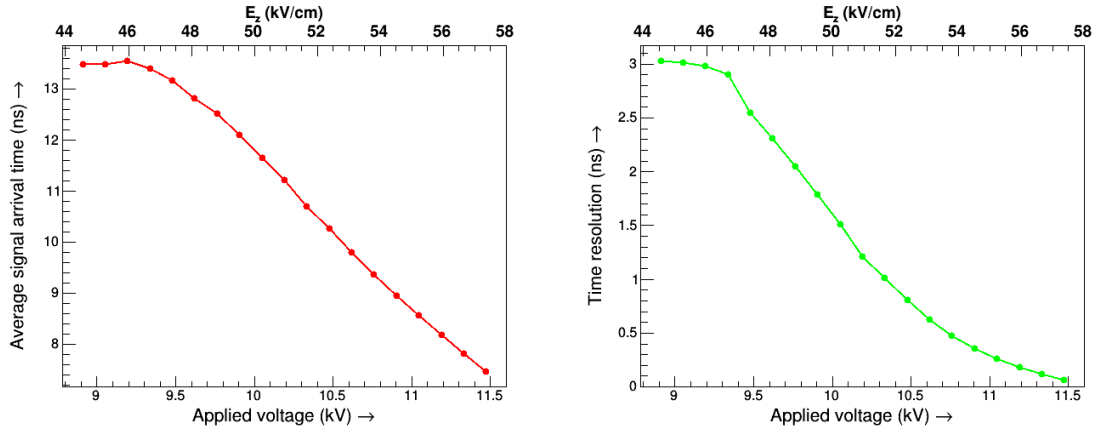


**Figure 6.** Variation of average signal arrival time and time resolution with the applied voltage found numerically for R-134A : Isobutane = 95 : 5.

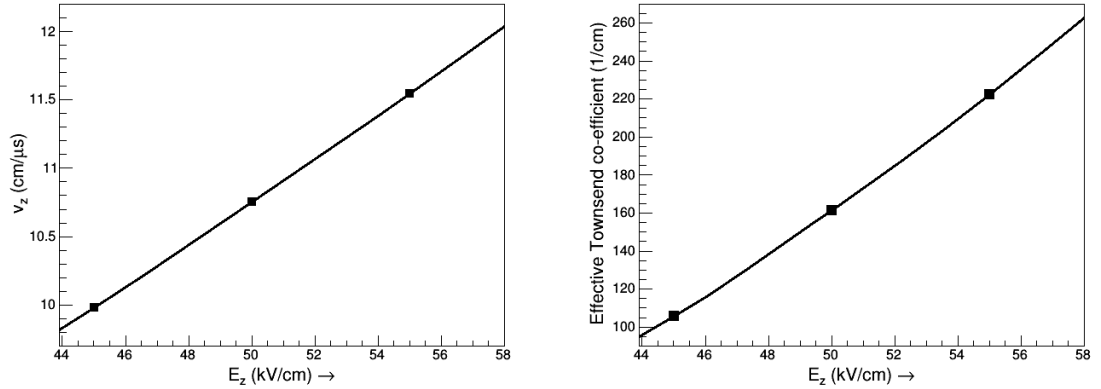


**Figure 7.** Variation of electron drift velocity ( $V_z$ ) and effective Townsend co-efficient of the gas mixture R-134A : Isobutane = 95 : 5 with  $E_z$ .

To see the effect of different geometrical components on the timing properties, a simplified approach has been taken where their effect on the drift of electrons has been determined.

Electrons have been released at different regions, all at a fixed distance (1.7 mm) from the bakelite plate on the side of anode and the time taken by them to reach the anode has been filled in a histogram. This calculation has been done keeping the applied voltage constant for which the value of  $E_z$  at a regular position is 42.76 kV/cm. The histograms of electron

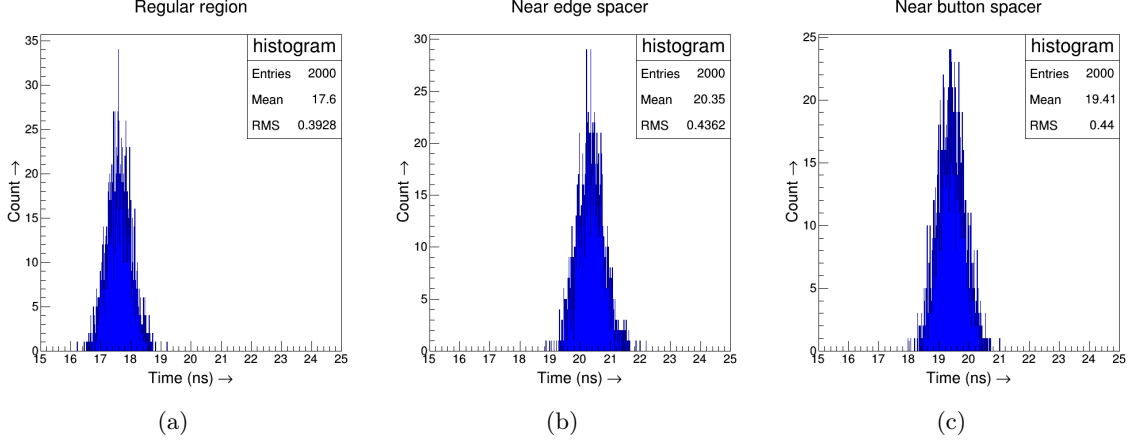


**Figure 8.** Timing histograms for (a) regular region, (b) 1 mm from edge spacer and (c) 200  $\mu$ m from the corner of pedestal part of the button spacer.

drift times for different regions are shown in figure 8. The mean of each distribution gives the average time taken by the electrons to reach the plate on which voltage of positive polarity has been applied. From the three histograms it can be seen that the electrons at 1 mm away from the edge spacer ( $E_z = 36.02$  kV/cm) take about 3 ns longer time whereas, the electrons at 200  $\mu$ m away from the corner of the pedestal part of the button spacer ( $E_z = 35.72$  kV/cm) take about 2 ns more in comparison to those drifting in the regular region. To see the effect of SF<sub>6</sub> on the timing properties, the same calculations have been performed for the gas mixtures R-134A : Isobutane : SF<sub>6</sub> = 95.0 : 4.5 (4.8, 4.9) : 0.5 (0.2, 0.1). The variation of the two timing parameters with the applied voltage and the corresponding value of  $E_z$  is shown in figure 9. A higher value of both average signal arrival time and time resolution has been found for higher amounts of SF<sub>6</sub> in the gas mixture which is at par with our earlier work [10].

## 4 Conclusion

The reduction of signal amplitude as one approaches the edge spacer can be attributed to the affected field configuration of those regions and will lead to loss of response decreasing the effective active area of a RPC.

The trend of variation in signal arrival time and time resolution with the applied voltage in simulation agrees with that obtained in experiment, although they differ quantitatively. Nevertheless, the present simulation produces time resolution values close to the analytical estimates [9]. The simulation will be improved in the future by considering the real-life factors of an experiment, to compare with the measurement. This will include the effect of movement of ions and electronic impedance on the signal shape. We also plan to take the

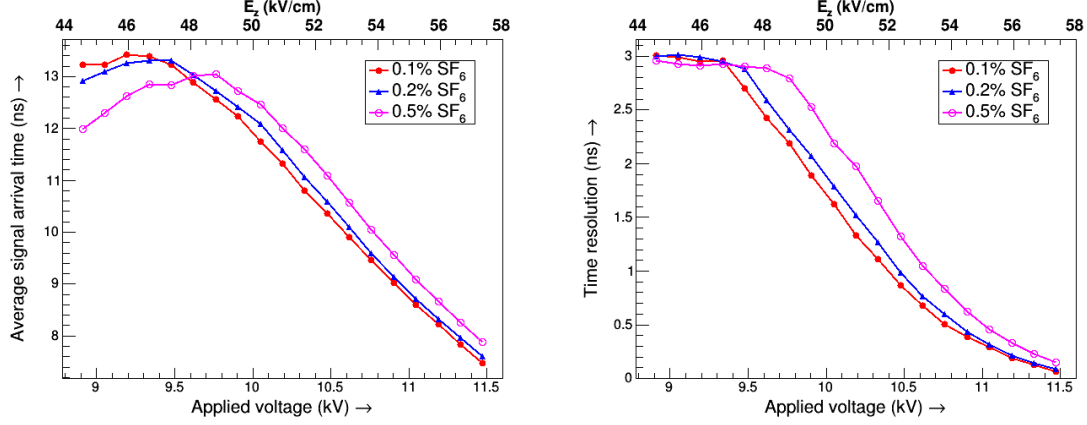


**Figure 9.** Variation of average signal arrival time and time resolution with the applied voltage for different SF<sub>6</sub> percentages.

finite bulk resistivity of the bakelite plates into account instead of treating them as perfect dielectrics.

Preliminary calculations have shown that electrons at the critical regions like near an edge or button spacer, takes more time compared to a region away from any imperfections. This may affect the timing response in those critical regions. The effect of these regions on the RPC time resolution following the present method of calculation by considering a current threshold will be investigated in the future.

The average signal arrival time has been found to increase with the amount of SF<sub>6</sub> present in the gas mixture. The present calculations have shown a deterioration in time resolution with the increase in SF<sub>6</sub> percentage.

## Acknowledgments

We would like to acknowledge the fruitful discussions with the INO collaboration and thank Purba Bhattacharya for her suggestions with the numerical calculations and Meghna K.K. for her help in the experimental measurements. We also thank the reviewer of this paper and the Editor for their constructive suggestions and help in improving the quality of the paper.

## References

- [1] ICAL collaboration  
*Physics Potential of the ICAL detector at the India-based Neutrino Observatory (INO)*,  
*arXiv:1505.07380*.
- [2] M. Bhuyan et al.  
*Cosmic ray test of INO RPC stack*, *Nucl. Instr. Meth. A* **661** (2012) S68.
- [3] C. Lippmann and W. Riegler  
*Space charge effects in Resistive Plate Chambers*, *Nucl. Instr. Meth. A* **517** (2004) 54-76.



- [4] A. Jash et al.  
*Numerical studies on electrostatic field configuration of Resistive Plate Chambers for the INO-ICAL experiment*, *jinst* **10** (2015) P11009.
- [5] Garfield : Rob Veenhof  
<http://garfield.web.cern.ch/garfield>.
- [6] N. Majumdar and S. Mukhopadhyay  
*Simulation of 3D electrostatic configuration in gaseous detectors*, *jinst* **2** (2007) P09006.
- [7] I.B. Smirnov  
*Modeling of ionization produced by fast charged particles in gases*, *Nucl. Instr. Meth. A* **554** (2005) 474-493.
- [8] S.F. Biagi  
*Accurate solution of the Boltzmann transport equation*, *Nucl. Instr. Meth. A* **273** (1988) 533.
- [9] W. Riegler and C. Lippmann  
*Detailed models for timing and efficiency in resistive plate chambers*, *Nucl. Instr. Meth. A* **508** (2003) 14-18.
- [10] M. Salim et al.  
*Simulation of efficiency and time resolution of resistive plate chambers and comparison with experimental data*, *jinst* **10** (2015) C04033.